Published in final edited form as:
Nano Lett. 2011 February 9; 11(2): 694–700. doi:10.1021/nl103812a.

Targeted Delivery of Nanoparticles to Ischemic Muscle for Imaging and Therapeutic Angiogenesis

Jaeyun Kim[†,⊥], **Lan Cao**[†,⊥], **Dmitry Shvartsman**[†], **Eduardo A. Silva**[†], and **David J. Mooney**[†,*]

[†]School of Engineering and Applied Sciences, and Wyss Institute, Harvard University, Cambridge, MA 02138

Abstract

Targeting of nanoparticles to ischemic tissues was studied in a murine ischemic hindlimb model. Intravenously injected fluorescent nanoparticles allowed ischemia-targeted imaging of ischemic muscles due to increased permeability of blood vessels in hypoxic tissues. Targeting efficiency correlated with blood perfusion after induction of ischemia and was enhanced in early stage of ischemia (<7 days). Therapeutic delivery of vascular endothelial growth factor (VEGF) was achieved by VEGF-conjugated nanoparticles and resulted in a 1.7-fold increase in blood perfusion, as compared to control mice. This work supports the application of nanoparticles as imaging and therapeutic modalities for ischemia treatment.

Keywords

Nanoparticles; VEGF; drug delivery; imaging; therapeutic angiogenesis; targeting

Targeting of diagnostic and therapeutic modalities to tumors using nanoparticles has emerged as a novel strategy in cancer research and therapy.[1–5] Recent studies have successfully demonstrated selective targeting of various nanoparticles including iron oxide,[6–12] semiconductors,[4,13–16] gold,[17–20] and biodegradable polymer[21–23] to tumors and other tissues. The potential advantages of nanoparticles in drug delivery include a minimization of nonspecific toxicity and an enhancement of therapeutic efficiency. Here, we introduce targeting of nanoparticles to ischemic muscle tissue for imaging or therapeutic angiogenesis of diseased muscle, via hypoxia-mediated enhanced vessel permeability.

Ischemia results from the obstruction of blood flow and can lead to cell damage in downstream tissues due to lack of oxygen and nutrients. Therapeutic angiogenesis, which aims to stimulate new blood vessel formation in ischemic tissues, is an attractive approach to treat ischemia,[24–26] and typically involves building new blood vessels via their sprouting and branching from existing vessels, a process termed angiogenesis. Therapeutic angiogenesis can be achieved by delivery of various growth factors, including vascular endothelial growth factor (VEGF).24–26 In clinical trials, VEGF has been delivered via bolus injections into either the ischemic site or the systemic circulation, but no significant

*To whom correspondence should be addressed. mooneyd@seas.harvard.edu.
⊥These authors contributed equally to this work

Supporting Information Available. Detailed experimental procedures, hydrodynamic size of bare silica nanoparticles, biodistribution of fluorescent nanoparticles, enlarged fluorescence images of cryosectioned ischemic and non-ischemic limbs injected with Cy-SiNPs, fluorescence images of opposite side of ischemic limbs after injection of Cy-SiNPs at 1, 3, 7, and 14 days post-induction of ischemia, TEM image of as-synthesized gold nanoparticles, and immunostained images of ischemic hindlimbs for CD31 straining. This material is available free of charge via the internet at http://pubs.acs.org.

improvements were achieved,[27–29] likely due to the short half-life of VEGF in circulation, no specific targeting, and the requirement for VEGF to be present for relatively long time periods (e.g., days-weeks) to prevent regression of the newly formed vessels.[30, 31] To overcome these limitation in current delivery, it is important to achieve delivery of VEGF specifically to ischemic tissue and maintain an elevated level for a sustained time. Recently, our group and others have shown that the encapsulation and local delivery of VEGF from biodegradable polymer hydrogels leads to significant recovery in animal models through sustained and localized release to the ischemic regions.[32–38] However, these materials require invasive local delivery into the tissue, and likely will also require multiple, appropriately spaced injections to target large or anatomically distinct regions of tissue ischemia in human patients.

An ideal solution for delivery of therapeutic angiogenic factors is their introduction into the blood stream, with subsequent targeting to ischemic regions. To address this, we recalled tumor-targeting strategy using nanoparticles. Research in the cancer field has demonstrated that blood vessels in tumors, due to their chronic overstimulation with tumor-secreted angiogenic factors, have increased vessel permeability that allows extravasation and accumulation of nanoparticles in the tumor tissue, which is known as the enhanced permeability and retention (EPR) effect.[2] Here we hypothesize that nanoparticles could be targeted to ischemic muscle via the EPR effect, as a similar angiogenic situation may exist in ischemic tissues. Ischemia in peripheral tissue leads to upregulated expression of a variety of angiogenic factors[39,40] that may enhance localized blood vessel permeability as they activate and mobilize endothelial cells in blood vessels. However, endogenous angiogenic factors are insufficient to promote recovery of large volumes of ischemic tissue, necessitating the delivery of exogenous VEGF to enhance the angiogenesis process.

To address this hypothesis, muscles was examined in a murine model of hindlimb ischemia, a standard model of peripheral artery disease (PAD).[41] Ligation of the femoral artery in one limb results in low blood perfusion in the entire hindlimb tissue, as observed using laser Doppler perfusion imaging (LDPI) (Figure 1a). As a model nanoparticular system, silica nanoparticles,[42, 43] were synthesized (~40 nm, Figure 1b) and doped with rhodamine B (R-SiNPs) or Cy5.5 (Cy-SiNPs) (Figure 1c). To increase the colloidal stability of the nanoparticles in circulation, their surface was modified with polyethylene glycol (PEG) through the condensation of the silane coupling agent with surface hydroxyl groups. Bare R-SiNPs rapidly precipitated in a saline solution, and their hydrodynamic size was in the range of 100 to 1000 nm (see Supporting Information, Figure S1). In contrast, PEGylated R-SiNPs showed a higher colloidal stability in saline, and a hydrodynamic size of 80 nm (Figure 1d), which in cancer research has been shown to be an appropriate size (< ~ 200 nm) to penetrate leaky blood vessels.[2]

To investigate if the nanoparticles can target the ischemic murine hindlimb tissue, bare and PEGylated R-SiNPs were injected intravenously 1 day post creation of ischemia. Fluorescent imaging of major organs demonstrated a high accumulation of bare nanoparticles in the reticuloendothelial system (RES), including the liver and spleen (see Supporting information Figure S2) as compared to a greatly reduced non-specific accumulation of PEGylated nanoparticles in these tissues (Figure S2), confirming past reports that PEGylation of the silica nanoparticles helps avoid RES entrapment and leads to more stable and longer-circulating particles.[43] The clear fluorescent signal in the bladder resulting from the PEGylated nanoparticles also indicated that the PEGylated nanoparticles can be excreted through the urine after circulation in the bloodstream.[43] Next, accumulation of nanoparticles in ischemic and normal hindlimbs was analyzed (Figure 2a and 2b). Very little accumulation in either site was noted with introduction of bare silica nanoparticles, likely due to the high level of entrapment of these particles in the RES after injection. In

contrast, introduction of PEGylated nanoparticles led to a high level of accumulation in ischemic hindlimbs, but not in normal limbs, suggesting PEGylated nanoparticles could substantially target to ischemic muscle. Fluorescence images of cryosectioned ischemic limbs also indicated a significant increase in deposition of nanoparticles in ischemic muscle fibers, as compared to non-ischemic tissue (Figure 2c, and see Supporting Information Figure S3 for enlarged images). This effect is presumably due to the secretion of multiple angiogenic factors in the ischemic tissue due to hypoxia[39, 40] and the resulting increased blood vessel permeability. Importantly, PEGylated nanoparticles were widely distributed throughout the entire ischemic tissue (Figure 2a and 2b), rather than being locally concentrated only around the site at which blood flow to the limb was interrupted. The observed broad and even distribution of nanoparticles in large regions of ischemic muscle tissue suggests that this approach can be used to deliver therapeutic molecules throughout a large tissue volume. In contrast, the bolus injections used in clinical trials and even discrete polymer hydrogel delivery systems would require multiple injections, and diffusion of the agent from each site of introduction into the surrounding tissue, likely leading to a heterogeneous tissue distribution. Nanoparticles have recently been demonstrated to concentrate at injured vasculature via targeting to highly expressed antigens;[21] the present approach, in contrast, promotes nanoparticle concentration within ischemic tissue via a physical mechanism (enhanced permeability).

The temporal window available to target nanoparticles to ischemic tissues was next examined (Figure 3a). PEGylated Cy-SiNPs were injected intravenously via tail vein injections into mice at various times post-induction of tissue ischemia, and the ischemic and normal hindlimbs were subsequently imaged. Qualitatively, a greater accumulation of nanoparticles was found with introduction of nanoparticles at early time points (1 and 3 day post-induction), and a gradual decrease at 7 and 14 days (Figure 3b, and see Supporting Information Figure S4 for fluorescent images of opposite side of limbs). At 14 days, the nanoparticle accumulation occurred mainly in the extremities of the ischemic limbs, where presumably natural recovery is slowest. Quantitative analysis of particle accumulation in the entire ischemic limb, relative to the matched normal limb, confirmed the qualitative findings (Figure 3c). To verify the reason of the decrease in accumulation of nanoparticles, we checked blood perfusion with LDPI for 14 days after induction of ischemia (Figure 3d and 3e). Blood perfusion to the effected limbs remained low for the entire 14 day time period, although perfusion slowly increased from 25% to 40% of normal values over this time period. This limited increase in perfusion over time represents the natural recovery in this mouse model due to endogenous angiogenesis and the enlargement of collateral arteries.[44, 45] Interestingly, there was an inverse relation between targeting of nanoparticles to the ischemic limb and blood perfusion levels (Figure 3c and 3d), as lower perfusion correlated with higher nanoparticle-targeting to ischemic tissue. The limited spontaneous recovery of perfusion will lead to increased oxygen concentration in the ischemic tissue, likely leading to a decreased local expression of angiogenic growth factors and vessel permeability. The levels of phosphorylated VEGF receptor 2 (VEGFR2), indicative of activated VEGF receptors and elevated endogenous levels of VEGF,[39,40] in the ischemic muscle tissue were also analyzed to confirm that ischemia did indeed result in local activation of endothelial cells. The level of phosphorylated VEGFR2 was greatest at days 1 and 3, was reduced by day 7, and largely absent by day 14 (Figure 3f), in support of a decreased level of tissue ischemia over time in this model. This finding of a temporal window for ischemia targeting with nanoparticles indicates the targeting of ischemic tissue is more time dependent than tumor targeting. The chronic angiogenesis found in tumors generates continuous leakiness in vessels around the tumor that can be used for nanoparticles targeting regardless of time. In contrast, administration of nanoparticles needs to be performed while tissues are still highly ischemic to get good efficiency for imaging and therapy.

The finding that nanoparticles home to ischemic tissues opens the possibility that nanoparticles can be used to deliver exogenous growth factors to drive therapeutic angiogenesis in these tissues. Recombinant human VEGF165 was selected as a potential therapeutic angiogenic factor due to its extensive history in preclinical and clinical trials.[27, 28, 32–34] Gold nanoparticles were selected as the delivery agent, as they have been utilized to bind therapeutic proteins with Au-thiol bonds without altering protein activity in tumor-targeted delivery.[46] The gold nanoparticles were prepared by citrate-reduction of Au^{3+} ions[47] and the size of gold nanoparticles was around 27 nm, as measured in TEM (see Supporting Information Figure S5). VEGF was conjugated to the surface of gold nanoparticles via coordinated covalent binding between the gold and the thiol group on cysteine residues in VEGF.[46] The hydrodynamic size of gold nanoparticles in saline increased from 67 to 124 nm after VEGF conjugation (Figure 4a), which was still less than the 200 nm diameter required for effective EPR effect.[2] TEM measurement of nanoparticle size was consistent with the nanoparticle size prior to conjugation and no significant aggregation was observed (Figure 4b). Only a small fraction of the bound VEGF (~3%) was released from the gold nanoparticles over 33 days in vitro (Figure 4c), indicating the stability of the covalent bonds between the gold and VEGF, and the suitability of the nanoparticles to bind VEGF as they circulate in the blood stream prior to accumulating in ischemic tissue. To confirm the bioactivity of VEGF conjugated with nanoparticles on endothelial cells, HMVEC-d were cultured with 50 ng/ml of free VEGF and the equivalent concentration of VEGF conjugated nanoparticles for 3 days, and the subsequent cell counts were normalized to no growth factor control (Figure 4d). Both VEGF and VEGF conjugated on nanoparticles led to higher endothelial cell proliferation than the no growth factor control, indicating the VEGF conjugated on nanoparticles maintained its ability to stimulate endothelial cell proliferation.

Next, the angiogenic response to intravenous injection of VEGF conjugated nanoparticles was analyzed via determination of capillary formation and blood perfusion in the hindlimb ischemia model. VEGF-conjugated gold nanoparticles were introduced into mice 1 day post induction of ischemia. The regional blood flow was abruptly reduced to ~ 30% of normal levels in all conditions after ischemic surgery, as expected (Figure 4e). No-treatment led to a slow increase in blood flow to the tissue over time. Delivery of free VEGF, mimicking the delivery approach in past clinical trials, resulted in no significant difference from the no-treatment control group. The injection of another control, PEGylated gold nanoparticles, also resulted in no significant difference from the no-treatment group (Figure S6). In contrast, VEGF-conjugated gold nanoparticles led to a recovery of blood perfusion over time to a level 93% of normal tissue, a 1.7-fold increase as compared with the blank condition at the end point of the study (Figure 4e). Quantification of blood vessel densities using immunohistochemical staining of tissues to CD31, an endothelial cell marker, revealed that delivery of VEGF conjugated nanoparticles increased capillary densities 2.6- and 2.0-fold, as compared with blank and bolus injection of VEGF, respectively (Figure 4f, see Supporting Information Figure S6 for representative images). Taken together, these results demonstrate that VEGF coupled to nanoparticles could be specifically and efficiently delivered to ischemic muscle tissue. These results also likely relate to the relatively even distribution of nanoparticles, and resulting drug delivery, throughout the entire ischemic tissue.

Finally, to confirm that the increased vascular permeability in ischemic tissue resulted from angiogenic factor stimulation, the tissue concentration of exogenous VEGF was artificially raised in non-ischemic tissues using previously described injectable hydrogel system.[32–34] One day later, fluorescent silica nanoparticles (R-SiNPs) were injected intravenously, and subsequently imaged. This experiment demonstrated a significant accumulation of the nanoparticles in the tissue stimulated with exogenous angiogenic factors (Figure 5a).

Injection of free VEGF (Figure 5b) and the hydrogel alone without VEGF (Figure 5c) did not lead to significant accumulation of nanoparticles in the same region of tissue. This finding supports the importance of sustained angiogenesis, such as that resulting from tissue ischemia, in promoting vessel permeability and nanoparticle accumulation. Strikingly, this last finding also suggests one may broadly target nanoparticles to virtually any tissue on demand for a window of time, in the absence of ischemia, simply by transiently creating permeable vessels via localized delivery of exogenous angiogenic factors.

In summary, nanoparticles conveying a payload for imaging and therapy can be targeted to ischemic muscle tissues via the EPR effect in the murine hindlimb ischemic model. Nanoparticles less than 200 nm in diameter demonstrated an increased accumulation in ischemic muscle. There was a temporal window within 7 days after induction of ischemia for highest targeting of nanoparticles. Severe hindlimb ischemia can be modulated by nanoparticles serving as carriers of exogenous VEGF, opening new possibilities for treating large and/or multiple ischemic tissues with this targeting approach and a variety of drugs.

Supplementary Material

Refer to Web version on PubMed Central for supplementary material.

Acknowledgments

This work was supported by the Wyss Institute for Biologically Inspired Engineering at Harvard University, National Institutes of Health Grant R01 HL069957, and EMBO Long-Term Fellowship ALTF 42-2008.

REFERENCES

1. Ferrari M. Nat. Rev. Cancer. 2005; 5:161–171. [PubMed: 15738981]
2. Peer D, Karp JM, Hong S, FaroKHzad OC, Margalit R, Langer R. Nat. Nanotechnol. 2007; 2:751–760. [PubMed: 18654426]
3. Cao YC, Jin R, Mirkin CA. Science. 2002; 297:1536–1540. [PubMed: 12202825]
4. Medintz IL, Uyeda HT, Goldman ER, Mattoussi H. Nat. Mater. 2005; 4:435–446. [PubMed: 15928695]
5. Rosi NL, Mirkin CA. Chem. Rev. 2005; 105:1547–1562. [PubMed: 15826019]
6. Bulte JW, Douglas T, Witwer B, Zhang SC, Strable E, Lewis BK, Zywicke H, Miller B, van Gelderen P, Moskowitz BM, Duncan ID, Frank JA. Nat. Biotechnol. 2001; 19:1141–1147. [PubMed: 11731783]
7. Na HB, Song IC, Hyeon T. Adv. Mater. 2009; 21:2133–2148.
8. Cheng K, Peng S, Xu CJ, Sun SH. J. Am. Chem. Soc. 2009; 131:10637–10644. [PubMed: 19722635]
9. Gao JH, Liang GL, Cheung JS, Pan Y, Kuang Y, Zhao F, Zhang B, Zhang XX, Wu EX, Xu B. J. Am. Chem. Soc. 2008; 130:11828–11833. [PubMed: 18681432]
10. Lee JH, Huh YM, Jun Y, Seo J, Jang J, Song HT, Kim S, Cho EJ, Yoon HG, Suh JS, Cheon J. Nat. Med. 2007; 13:95–99. [PubMed: 17187073]
11. Mulder WJM, Strijkers GJ, van Tilborg GAF, Griffioen AW, Nicolay K. NMR Biomed. 2006; 19:142–164. [PubMed: 16450332]
12. Gao J, Gu H, Xu B. Acc. Chem. Res. 2009; 42:1097–1107. [PubMed: 19476332]
13. Choi HS, Liu WH, Liu FB, Nasr K, Misra P, Bawendi MG, Frangioni JV. Nat. Nanotechnol. 2010; 5:42–47. [PubMed: 19893516]
14. Kim S, Lim YT, Soltesz EG, De Grand AM, Lee J, Nakayama A, Parker JA, Mihaljevic T, Laurence RG, Dor DM, Cohn LH, Bawendi MG, Frangioni JV. Nat. Biotechnol. 2004; 22:93–97. [PubMed: 14661026]

15. Michalet X, Pinaud FF, Bentolila LA, Tsay JM, Doose S, Li JJ, Sundaresan G, Wu AM, Gambhir SS, Weiss S. Science. 2005; 307:538–544. [PubMed: 15681376]
16. Mulder WJM, Koole R, Brandwijk RJ, Storm G, Chin PTK, Strijkers GJ, Donega CD, Nicolay K, Griffioen AW. Nano Lett. 2006; 6:1–6. [PubMed: 16402777]
17. Lal S, Clare SE, Halas NJ. Acc. Chem. Res. 2008; 41:1842–1851. [PubMed: 19053240]
18. Cobley CM, Chen J, Cho EC, Wang LV, Xia Y. Chem. Soc. Rev. 2011 Advanced Article.
19. Jain PK, Huang X, El-Sayed IH, El-Sayed MA. Acc. Chem. Res. 2008; 41:1578–1586. [PubMed: 18447366]
20. Popovtzer R, Agrawal A, Kotov NA, Popovtzer A, Balter J, Carey TE, Kopelman R. Nano Lett. 2008; 8:4593–4596. [PubMed: 19367807]
21. Chan JM, Zhang LF, Tong R, Ghosh D, Gao WW, Liao G, Yuet KP, Gray D, Rhee JW, Cheng JJ, Golomb G, Libby P, Langer R, Farokhzad OC. Proc. Natl. Acad. Sci. U.S.A. 2010; 107:2213–2218. [PubMed: 20133865]
22. Farokhzad OC, Cheng JJ, Teply BA, Sherifi I, Jon S, Kantoff PW, Richie JP, Langer R. Proc. Natl. Acad. Sci. U.S.A. 2006; 103:6315–6320. [PubMed: 16606824]
23. Torchilin VP. Nat. Rev. Drug Discov. 2005; 4:145–160. [PubMed: 15688077]
24. Diaz-Sandoval LJ, Losordo DW. Exp. Opin. Biol. Ther. 2003; 3:599–616.
25. Freedman SB, Isner JM. Ann. Int. Med. 2002; 136:54–71. [PubMed: 11777364]
26. Simons M, Ware JA. Nat. Rev. Drug Discov. 2003; 2:863–871. [PubMed: 14668807]
27. Simons M, Annex BH, Laham RJ, Kleiman N, Henry T, Dauerman H, Udelson JE, Gervino EV, Pike M, Whitehouse MJ, Moon T, Chronos NA. Circulation. 2002; 105:788–793. [PubMed: 11854116]
28. Henry TD, Annex BH, McKendall GR, Azrin MA, Lopez JJ, Giordano FJ, Shah PK, Willerson JT, Benza RL, Berman DS, Gibson CM, Bajamonde A, Rundle AC, Fine J, McCluskey ER, Investigators V. Circulation. 2003; 107:1359–1365. [PubMed: 12642354]
29. Lederman RJ, Mendelsohn FO, Anderson RD, Saucedo JF, Tenaglia AN, Hermiller JB, Hillegass WB, Rocha-Singh K, Moon TE, Whitehouse MJ, Annex BH, Investigators T. Lancet. 2002; 359:2053–2058. [PubMed: 12086757]
30. Eppler SM, Combs DL, Henry TD, Lopez JJ, Ellis SG, Yi JH, Annex BH, McCluskey ER, Zioncheck TF. Clin. Pharmacol. Ther. 2002; 72:20–32. [PubMed: 12152001]
31. Yancopoulos GD, Davis S, Gale NW, Rudge JS, Wiegand SJ, Holash J. Nature. 2000; 407:242–248. [PubMed: 11001067]
32. Silva EA, Mooney DJ. J. Thromb. Haemost. 2007; 5:590–598. [PubMed: 17229044]
33. Borselli C, Storrie H, Benesch-Lee F, Shvartsman D, Cezar C, Lichtman JW, Vandenburgh HH, Mooney DJ. Proc. Natl. Acad. Sci. U.S.A. 2010; 107:3287–3292. [PubMed: 19966309]
34. Lee J, Bhang SH, Park H, Kim BS, Lee KY. Pharm. Res. 2010; 27:767–774. [PubMed: 20221675]
35. Sun QH, Silva EA, Wang AX, Fritton JC, Mooney DJ, Schaffler MB, Grossman PM, Rajagopalan S. Pharm. Res. 2010; 27:264–271. [PubMed: 19953308]
36. Patel ZS, Ueda H, Yamamoto M, Tabata Y, Mikos AG. Pharm. Res. 2008; 25:2370–2378. [PubMed: 18663411]
37. Patel ZS, Mikos AG. J. Biomater. Sci. Polym. Ed. 2004; 15:701–726. [PubMed: 15255521]
38. DeVolder RJ, Kong HJ. Biomaterials. 2010; 31:6494–6501. [PubMed: 20538334]
39. Isner JM. J. Clin. Invest. 2000; 106:615–619. [PubMed: 10974011]
40. Semenza GL. J. Cell. Biochem. 2007; 102:840–847. [PubMed: 17891779]
41. Couffinhal T, Silver M, Kearney M, Sullivan A, Witzenbichler B, Magner M, Annex B, Peters K, Isner JM. Circulation. 1999; 99:3188–3198. [PubMed: 10377084]
42. He XX, Nie HL, Wang KM, Tan WH, Wu X, Zhang PF. Anal. Chem. 2008; 80:9597–9603. [PubMed: 19007246]
43. Burns AA, Vider J, Ow H, Herz E, Penate-Medina O, Baumgart M, Larson SM, Wiesner U, Bradbury M. Nano Lett. 2009; 9:442–448. [PubMed: 19099455]
44. Carmeliet P. Nat. Med. 2000; 6:389–395. [PubMed: 10742145]
45. Helisch A, Schaper W. Microcirculation. 2003; 10:83–97. [PubMed: 12610665]

46. Powell AC, Paciotti GF, Libutti SK. Methods Mol. Biol. 2010; 624:375–384. [PubMed: 20217609]
47. Enustun BV, Turkevich J. J. Am. Chem. Soc. 1963; 85:3317–3328.

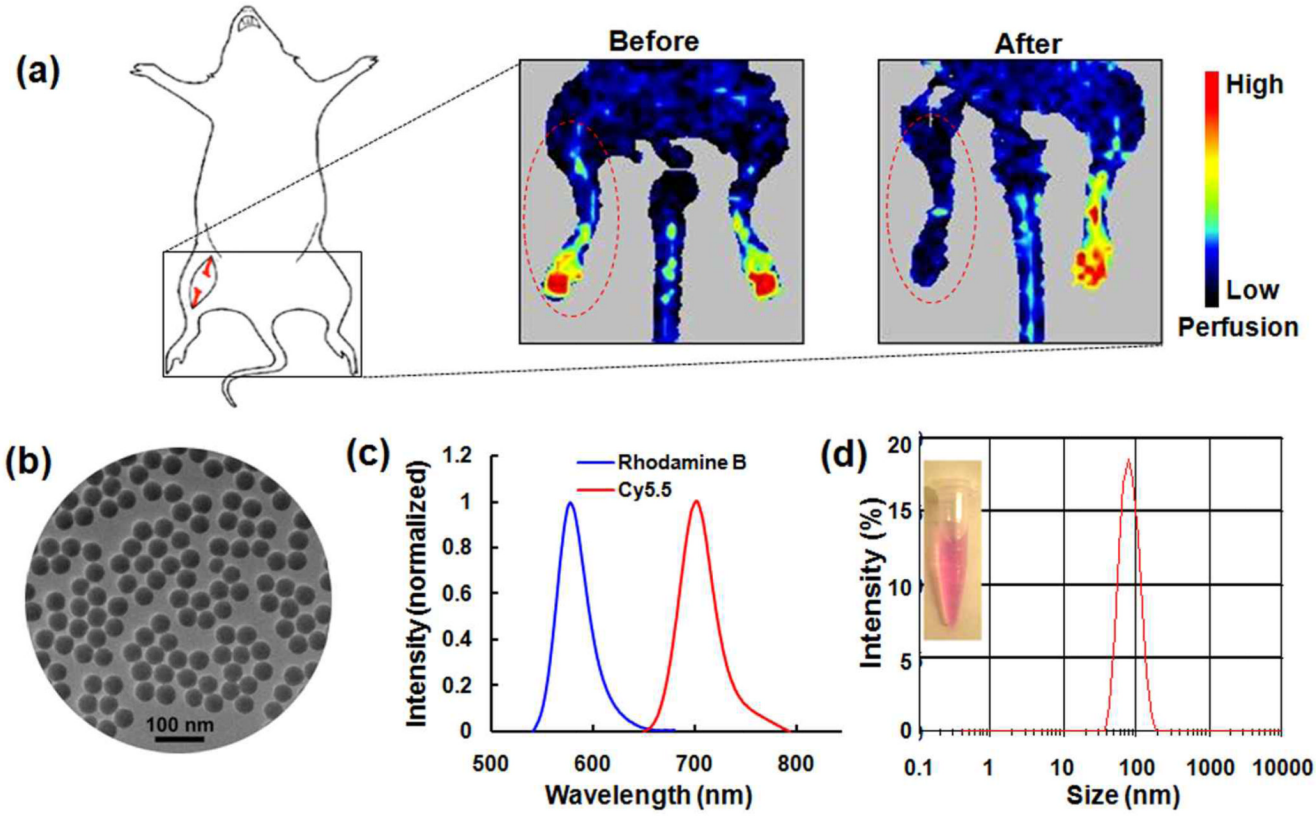

Figure 1.

Ischemic hindlimb model and fluorescent silica nanoparticles. (a) Laser Doppler perfusion imaging (LDPI) of murine ischemic hindlimb model before and after induction of ischemia. Ischemia was created in the limb encircled by the red dotted line, and LDPI images show the abrupt decrease in blood perfusion after induction. (b) A representative transmission electron microscope (TEM) image of fluorescent silica nanoparticles. (c) Photoluminescence spectra of rhodamine B- and Cy5.5- doped silica nanoparticles. (d) Hydrodynamic size of PEGylated silica nanoparticles in saline measured by dynamic light scattering (DLS). Inset photographs demonstrate the solution stability of the nanoparticles in PBS.

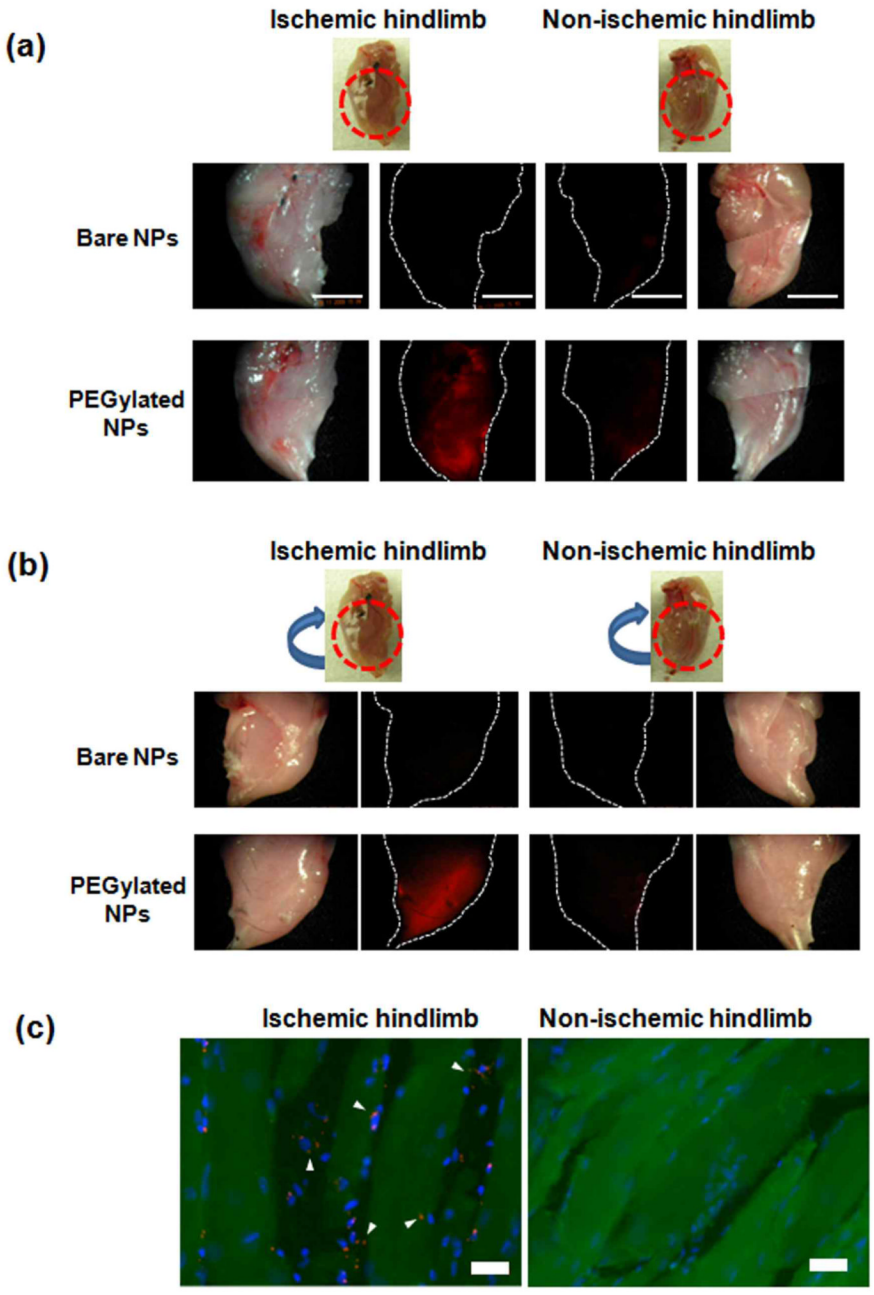

Figure 2.

Targeting of fluorescent nanoparticles to ischemic muscles. (a) Fluorescence images of ischemic and non-ischemic limbs after i.v. injection of nanoparticles. Photographs of limbs are presented as well. Scale bars: 5 mm. (b) Fluorescence images of opposite sides of ischemic and non-ischemic limbs. (c) Fluorescence images of cryosectioned ischemic (left) and non-ischemic (right) limb. Nanoparticles (Cy-SiNPs) are red. Nuclei were stained with 4',6-diamidino-2-phenylindole (DAPI) and are blue. Muscle fibers appear green due to autofluorescence (For enlarged image, see Supporting Information Figure S1). Scale bars: 20 μm.

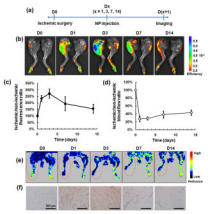

Figure 3.

Temporal window for targeting nanoparticles to ischemic tissue. (a) Time-table for induction of ischemia, nanoparticle injection, and fluorescence imaging. Nanoparticles (Cy-SiNPs) were injected 1, 3, 7, and 14 days post-induction of ischemia (n=3). (b) Representative fluorescent images of ischemic (left limb) and non-ischemic (right limb) condition at each time point. (c) Quantitative analysis of nanoparticle accumulation in the ischemic limb, as a ratio of accumulation in the matched non-ischemic limb. (d) Quantitative analysis of tissue perfusion as a function of time, normalized to the contralateral non-ischemic limb. (e) Representative images of perfusion in hindlimbs as a function of time; each image corresponds to the time point in Figure 3d, and demonstrates the limited spontaneous recovery of perfusion in this model. Again, both ischemic (left limb, red dotted circles) and contralateral control (right limb) are shown at each time point. (f) Representative photomicrographs from tissue sections of the ischemic hindlimb muscle tissue following immunohistochemical staining for phosphorylated VEGFR2. Values in (c) and (d) represent mean and standard deviation.

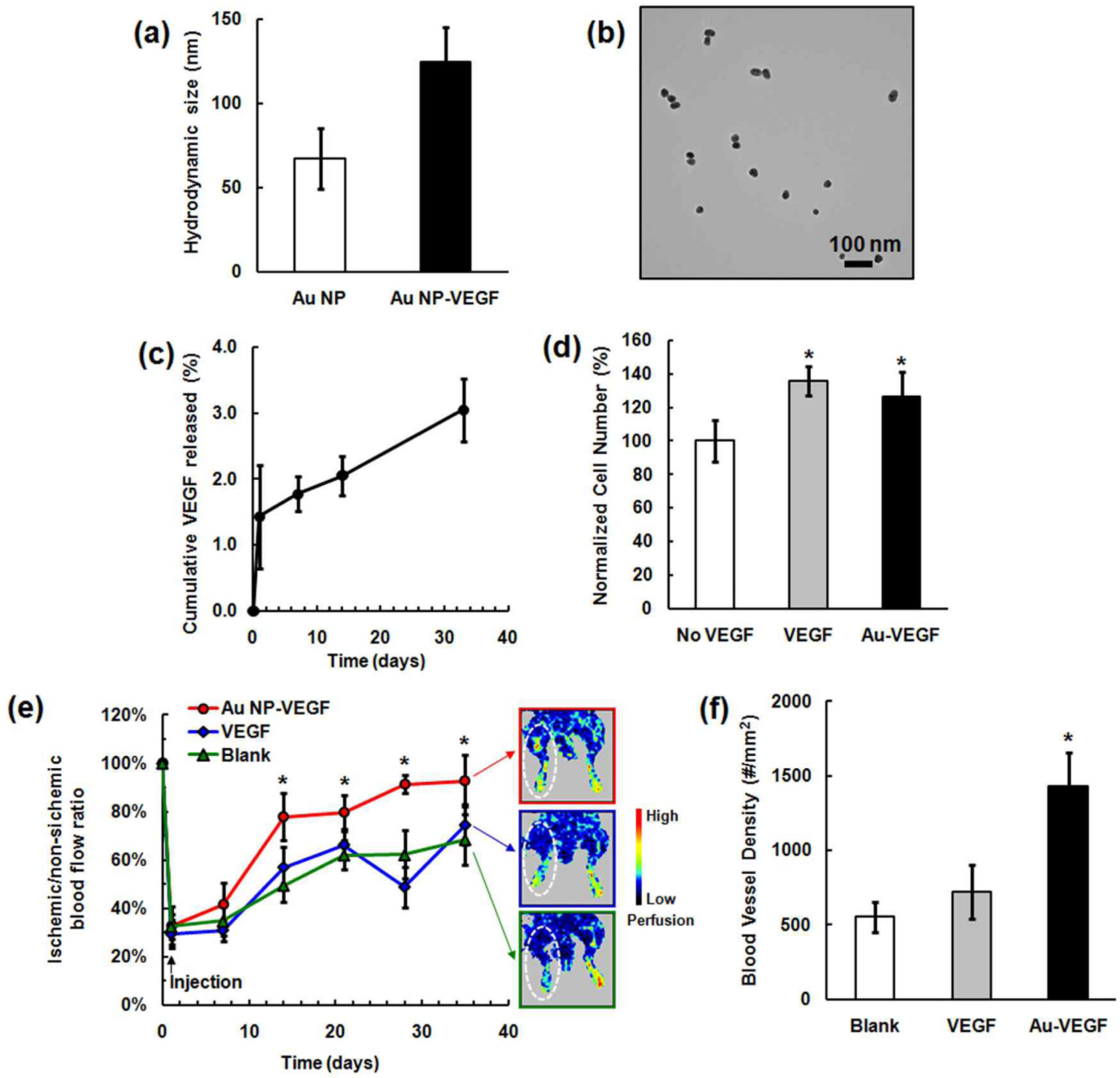

Figure 4.

Therapeutic angiogenesis using delivery of exogenous VEGF conjugated to nanoparticles. (a) Hydrodynamic size of gold nanoparticles before and after conjugation with VEGF. (b) TEM image of VEGF-conjugated gold nanoparticles (4.9 mg/ml), demonstrating little aggregation after conjugation. (c) Cumulative in vitro release profile of VEGF from gold nanoparticles. (d) The proliferation of human microvascular endothelial cells (HMVEC-d) after 72 h of culture without VEGF, with 50 ng/ml of free VEGF, and VEGF conjugated gold nanoparticles corresponding to 50 ng VEGF/ml. (e) Quantitative analysis of tissue blood perfusion over 5 weeks in ischemic limbs with injection of VEGF conjugated gold nanoparticles (Au NP-VEGF), free VEGF injection (VEGF), and no treatment (Blank) (n=8). *, statistically significant difference ($P<0.05$), as compared with controls (Blank and

VEGF). Inset: representative LDPI images of each condition at end point. (f) Quantification of capillary densities in hindlimb muscle tissues at 5 weeks with injection of Au NP-VEGF, free VEGF, and no treatment (Blank). Values in (c), (d), (e) and (f) represent mean and standard deviation.

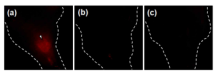

Figure 5.
Triggering vessel permeability to deliver nanoparticles. Fluorescent images of non-ischemic limbs following nanoparticle delivery with prior direct injection into the non-ischemic hindlimb tissue of (a) VEGF-loaded alginate hydrogel, (b) free VEGF, and (c) alginate hydrogel without VEGF.